PREMIER COLLOQUE IMAGE
Traitement, Synthèse, Technologie et Applications
BIARRITZ — Mai 1984 —

TOMOGRAPHIC IMAGE RECONSTRUCTION FROM INCOMPLETE DATA BY USING CONVEX PROJECTIONS AND DIRECT FOURIER INVERSION

RECONSTRUCTION TOMOGRAPHIQUE A PARTIR DE DONNEES INCOMPLETES PAR PROJECTION CONVEXE ET INVERSION DIRECTE DE FOURIER

M. Ibrahim Sezan and Henry Stark

ECSE Department, Rensselaer Polytechnic Institute, Troy, N.Y. 12181, USA

RESUME

Dans cet article on considère le problème de la reconstruction des images tomographiques aideés par l'ordinateur (apellé CAT) par la méthode directe de Fourier (apellé DFM) à partir de données incomplètes de la vue. On utilise la méthode de projection sur les ensembles convexes (apellé POCS) pour rétablir les données absentes de la vue. POCS est une technique récurrente du rétablissement de l'image qui trouve une solution consistente avec les données mesurées et les constraintes connues *à priori* dans les domaines de Fourier et de l'espace.

On concoit et applique un algorithme (PRDF) qui interpole/extrapole l'information absente de la domaine de Fourier par POCS et reconstruit une image par DFM. Une vue en coupe du thorax humain est rétablie et reconstruite par les données de la projection simuleé des rayons X. Les rétablissements obtenus en utilisant POCS sont comparés avec la méthode d'extrapolation classique de Gerchberg-Papoulis et démonstrés à être superieurs. Les applications de PRDF aux tomographies résonnantes magnétiques nucléaires (appellé NMR) sont aussi discutées.

SUMMARY

In this paper we consider the problem of reconstructing computer aided tomography (CAT) imagery by the direct Fourier method (DFM) when not all view data is available. To restore the missing view data we use the method of projections onto convex sets (POCS). POCS is a recursive image restoration technique that finds a solution consistent with the measured data and *a priori* known constraints in both the space and Fourier domain.

We design and apply an algorithm (PRDF) which interpolates/extrapolates the missing Fourier domain information by POCS and reconstructs an image by Fourier inversion. A human thorax cross-section is restored and reconstructed from simulated X-ray projection data. The restorations using POCS are compared with the classical Gerchberg-Papoulis extrapolation method and shown to be superior. Applications of PRDF to nuclear magnetic resonance tomography are discussed.

M. Ibrahim Sezan and Henry Stark

TOMOGRAPHIC IMAGE RECONSTRUCTION FROM INCOMPLETE DATA BY USING CONVEX PROJECTIONS AND DIRECT FOURIER INVERSION
RECONSTRUCTION TOMOGRAPHIQUE A PARTIR DE DONNEES INCOMPLETES PAR PROJECTION CONVEXE ET INVERSION DIRECTE DE FOURIER

I. INTRODUCTION

In this paper we combine the direct Fourier method (DFM) of reconstructing from projections with an iterative restoration algorithm called the method of projections† onto convex sets (POCS) to reconstruct good quality imagery from incomplete projection (view) data. The method of POCS was discussed in [1] and [2] as applied to image restoration when only partial frequency or space domain data was available to reconstruct an arbitrary image. Tuy [3] used POCS to restore missing projection data in connection with reconstruction via filtered convolution back-projection (FCBP). However, since constraints are generally applied to the image or its spectrum (but not its projections) we are motivated to study the reconstruction from incomplete projection data problem from a different viewpoint. Why DFM/POCS? With regard to the method of restoration POCS offers two noteworthy advantages: (i) it enables any number of *a priori* convex-type constraints to be incorporated in the algorithm; and (ii) it guarantees convergence: weak in general, strong in practice. Having chosen POCS as the restoration algorithm, the logical reconstruction method is the direct Fourier method (DFM). Not only is DFM fast as a reconstruction algorithm but because it involves transformations between space and Fourier domains, it enables space-domain and Fourier-domain constraints to be applied in their respective spaces directly. Finally because exact interpolation formulas exist, DFM-reconstructed image can be made of same quality as by the method of filtered convolution back projection (FCBP).

II. REVIEW OF POCS

The function to be restored, $f(x,y)$ is assumed to be an element of a Hilbert space H which is the space of functions satisfying

$$\iint_{\Omega} |f(x,y)|^2 \, dxdy < \infty \tag{1}$$

with inner product

$$(f,g) \triangleq \iint_{\Omega} f(x,y)\, g^*(x,y)\, dxdy \quad ; \quad (f,g\varepsilon H) \tag{2}$$

and induced norm

$$||f|| \triangleq [(f,f)]^{1/2}. \tag{3}$$

The basic idea of POCS is as follows: Every known property of the unknown $f\varepsilon H$ will restrict f to lie in a closed convex set C_i in H. Thus, for m known properties there are m closed convex sets C_i, $i=1,2,\ldots,m$ and $f\varepsilon C_o \triangleq \bigcap_{i=1}^{m} C_i$. Then the problem is to find a point of C_o given the sets C_i and projection operators P_i projecting onto C_i, $i=1,2,\ldots,m$. The convergence properties of the sequence $\{f_k\}$ generated by the recursion relation

$$f_{k+1} = P_m P_{m-1} \cdots P_1 f_k \quad ; \quad k=0,1,\ldots \tag{4}$$

or more generally by

$$f_{k+1} = T_m T_{m-1} \cdots T_1 f_k \quad ; \quad k=0,1,\ldots \tag{5}$$

with $T_i \triangleq I+\lambda_i(P_i-I)$; $0<\lambda_i<2$, are based on fundamental theorems given by Opial [4] and Gubin et. al. [5]. The λ_i's, $i=1,\ldots,m$ are relaxation parameters and can be used to accelerate the rate of convergence of the algorithm. However, the λ's that are effective in the absence of noise will often be ineffective when noise is present [6]. Thus a single set of λ's is not effective at all signal-to-noise ratios. The following sets and their associated projection operators are among the ones used in Refs. [2] and [6] and they will be used here.

1. C_1: The set of all functions in H that vanish a•e outisde a prescribed region $S\subset\Omega$. Given an arbitrary f in H its projection onto C_1 is realized by

$$P_1 f = \begin{cases} f, & (x,y)\varepsilon S \\ 0, & (x,y)\notin S \end{cases} \tag{6}$$

2. C_2: The set of all functions in H whose Fourier transforms assume a prescribed value G over a closed region L in the u-v Fourier plane. The projection of an arbitrary f in H is realized by

$$P_2 f = \begin{cases} G(u,v), & (u,v)\varepsilon L \\ F(u,v), & (u,v)\notin L \end{cases} \tag{7}$$

where $F(u,v)=\mathcal{F}[f(x,y)]$ and $\mathcal{F}$ is the Fourier transform operator. In the case of incomplete view data $G(u,v)$ is known in a data cone with subtended angle of less than 180 degrees.

3. C_3: The set of all real valued nonnegative functions in H that satisfy the energy constraint

$$\iint_{\Omega} |f(x,y)|^2 \, dxdy \le E \triangleq \rho^2 \tag{8}$$

The projection of an arbitrary $f\varepsilon H$ onto C_3 is realized by

$$P_3 f = \begin{cases} 0, & f_1 < 0 \\ f_1^+, & E_1^+ \le E \\ \sqrt{\dfrac{E}{E_1^+}}\, f_1^+, & E_1^+ > E \end{cases} \tag{9}$$

where f_1 is the real part of f, f_1^+ is the rectified portion of f_1, and E_1^+ is the energy in f_1^+; i.e.,

$$E_1^+ \triangleq \iint_{\Omega} (f_1^+)^2 \, dxdy. \tag{10}$$

4. C_4: The set of all real valued functions in H whose amplitudes must lie in a prescribed closed interval $[a,b]$; $a\ge 0$, $b>0$, $a<b$. The projection of an arbitrary $f\varepsilon H$ onto C_4 is realized by the following rule

$$P_4 f = \begin{cases} a, & f(x,y) < a \\ f(x,y), & a \le f(x,y) \le b \\ b, & f(x,y) > b \end{cases} \tag{11}$$

Operators P_1, P_2, P_3 and P_4 were used in Eqs. (4) and (5) in restoring an image from its noiseless partial frequency spectrum [2]. They were also used together with a noise smoothing operator to restore images from noisy partial frequency spectrum [6]. In all cases the method of POCS outperformed the Gerchberg-Papoulis (G-P) algorithm [7].

III. REVIEW OF THE DIRECT FOURIER METHOD (DFM) OF RECONSTRUCTION FROM PROJECTIONS

The DFM is based on the central slice projection theorem [8]. Let $\mu(x,y)$ represent a function whose image is desired (e.g. in CAT, $\mu(x,y)$ is the X-ray absorptivity). Let $\mu_\phi(\hat{x},\hat{y})$ represent the same dis-

† Projections in the mathematical sense.

M. Ibrahim Sezan and Henry Stark

TOMOGRAPHIC IMAGE RECONSTRUCTION FROM INCOMPLETE DATA BY USING CONVEX PROJECTIONS AND DIRECT FOURIER INVERSION

RECONSTRUCTION TOMOGRAPHIQUE A PARTIR DE DONNEES INCOMPLETES PAR PROJECTION CONVEXE ET INVERSION DIRECTE DE FOURIER

tribution in a coordinate system $\hat{x}$-$\hat{y}$ rotated from x-y by an angle ϕ. The projection data at view angle ϕ is defined as

$$p_\phi(\hat{x}) \triangleq \int_L \mu_\phi(\hat{x},\hat{y})\, d\hat{y} \qquad (12)$$

where L is the beam path. The central slice projection theorem states that

$$P_\phi(\rho) = M(\rho,\phi) \qquad \rho\geq 0 \quad 0<\phi\leq 2\pi \qquad (13a)$$

where

$$P_\phi(\rho) = \int_{-\infty}^{\infty} p_\phi(\hat{x}) e^{-2\pi\rho\hat{x}} d\hat{x} \qquad (13b)$$

and $M(\rho,\phi)$ denotes the 2-D Fourier transform of the cross-section distribution $\mu(x,y)$ in polar coordinates. In practice $p_\phi(\hat{x})$ is the data actually obtained at the location of detectors $\{x_l\}$. In place of Eq. (13b) the discrete Fourier transform is used to obtain $P_\phi(\rho)$ at the discrete set of spatial frequencies $\{\rho_n\}$. Since the view angles are also a discrete set $M(\rho,\phi)$ is known at points on a polar grid $\{\rho_n,\phi_k\}$, $n=1,2,\ldots,N$; $k=1,2,\ldots,2K+2$ where N is the number of detectors, K is the highest harmonic in the angularly band-limited image and $\phi_k = \frac{2\pi}{2K+2}k$. We immediately see that if we could compute the 2-D inverse Fourier transform of $M(\rho_n,\phi_k)$ we would obtain the desired image.

At this point, direct Fourier methods require interpolating $M(\rho_n,\phi_k)$ to $M_c(u_\ell,v_m)$ where $M_c(\cdot)$ is the Fourier transform of $\mu(x,y)$ on a Cartesian raster. The interpolation from a polar to Cartesian raster is required in order to use the FFT routine. However, inexact interpolation is a major source of error in reconstruction by direct Fourier methods even when the interpolation errors are not large [9].

Recently an exact interpolation method was discussed [8, 10, 11] which, in direct comparisons, produced images equal or superior in quality to convolution back-projection methods. The method is based on the exact polar sampling theorem

$$M(\rho,\phi) = \sum_{n=-\infty}^{\infty} \sum_{k=0}^{\infty} M\left(\frac{n}{2A},\frac{\pi k}{K+1}\right) \mathrm{sinc}\left[2A\left(\rho-\frac{n}{2A}\right)\right]\sigma\left(\phi-\frac{\pi k}{K+1}\right) \qquad (14a)$$

where 2A is the diameter that bounds the object in space, K is the highest angular frequency in the periodic function $M(\rho,\phi)$ and $\sigma(\phi)$ is an azimuthal interplating function given by

$$\sigma(\phi) \triangleq \frac{\sin[(N/2)\phi]}{N\sin[(1/2)\phi]} \qquad (14b)$$

In practice a truncated interpolation involving a finite number of cardinal functions, truncated cardinal function expansion (TCFE), is used. Thus Eq. (14a) is replaced by

$$\hat{M}(\rho,\phi) = \sum_{n=n_\rho-L_\rho}^{n_\rho+L_\rho} \sum_{k=k_\phi-L_\phi}^{k_\phi+L_\phi} M\left(\frac{n}{2A},\frac{\pi k}{K+1}\right) \cdot \mathrm{sinc}\left(2A\left(\rho-\frac{n}{2A}\right)\right)\sigma\left(\phi-\frac{\pi k}{K+1}\right) \qquad (15)$$

where $[2A\rho]\triangleq n_\rho$ and $[(K+1)\phi/\pi]\triangleq k_\phi$, are the nearest neighbors to the point about which the expansion is done. In practice, image quality is improved when the truncation is tapered. The taper normally used is the Cartesian product of two identical one-dimensional triangular windows, $\omega(n)$, of the form

$$\omega(n) = \max(1-|n|/M,\ 0) \quad ; \quad n=0,\pm1,\pm2,\ldots \qquad (16)$$

$M=\infty$ is the abrupt truncation case. It is possible to adjust the relative proportions of radial and azimuthal interpolation by adjusting the quantities L_ρ and L_ϕ respectively. In this paper we use TCFE interpolation with tapering (M=5).

After interpolating the 2-D Fourier spectrum from a polar to a Cartesian raster, a 2-D inverse FFT is computed to obtain the desired image. The direct Fourier method is illustrated in Figure 1.

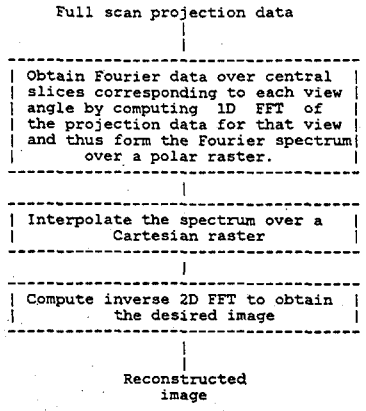

Figure 1. Direct Fourier inversion method (DFM)

IV. PRDF ALGORITHM

If projection data is available over a limited angular range, then the image Fourier transform $M(\rho,\phi)$ can be interpolated over a Cartesian grid within this angular range. The pixels remaining outside this angular range are set to zero as a first approximation. The missing frequency information is then restored by POCS and the desired image is obtained by inverse transforming. The complete algorithm is called PRDF and illustrated in Figure 2.

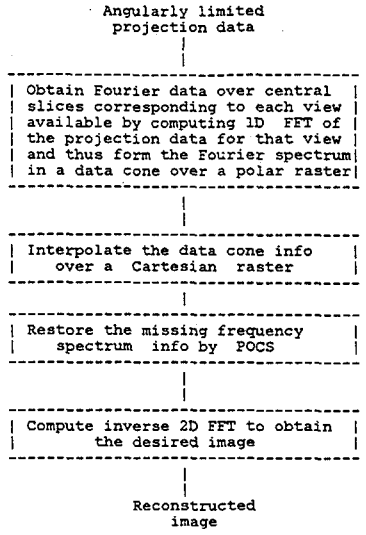

Figure 2. PRDF algorithm for reconstructing from angularly limited view data.

V. RECONSTRUCTING A THORAX PHANTOM FROM ANGULARLY-LIMITED X-RAY PROJECTION DATA

The simulated parallel beam projection data assumes an X-ray energy of 70 Kev, 128 detectors which are spaced apart by 0.3 cm. and 360 views over 360 de-

M. Ibrahim Sezan and Henry Stark

TOMOGRAPHIC IMAGE RECONSTRUCTION FROM INCOMPLETE DATA BY USING CONVEX PROJECTIONS AND DIRECT FOURIER INVERSION

RECONSTRUCTION TOMOGRAPHIQUE A PARTIR DE DONNEES INCOMPLETES PAR PROJECTION CONVEXE ET INVERSION DIRECTE DE FOURIER

grees. The interpolated transform with $L_\rho=3$, $L_\phi=1$, i.e., 21 interpolation points and resulting reconstruction of the thorax phantom from complete view data is shown in Figure 3.

Reconstruction by PRDF from angularly limited projection data is attempted for the following three cases; projection data is limited to the view range of i) [-80°,80°], ii) [-67°,67°], iii) [-45°,45°] (projection data missing about vertical axis). The formula of Eq. (15) with $L_\rho=3$, $L_\phi=1$ is used to interpolate $\hat{M}(\rho,\phi)$ from polar to Cartesian points. The Fourier transform for full-view data and the above three cases is shown after interpolation in Figure 4.

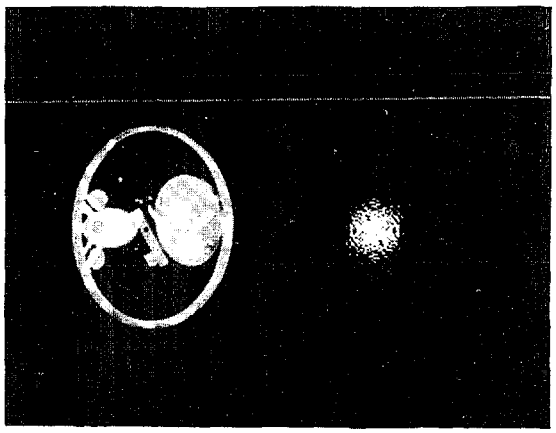

Figure 3. DFM reconstruction and interpolated spectrum.

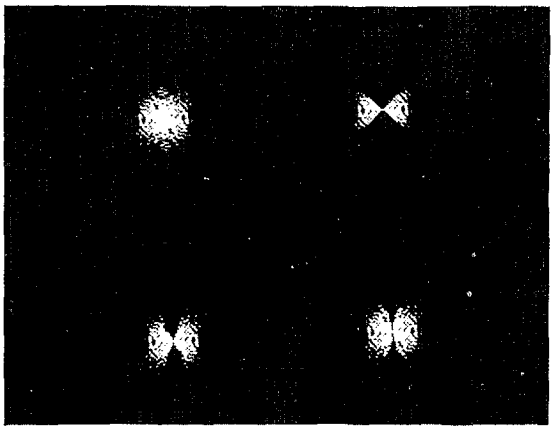

Figure 4. Interpolated frequency spectrum: Clockwise from upper left: full view projection data, view limited to [-45°,45°], view limited to [-80°,80°], view limited to [-67°,67°].

Results

The basis for comparing results was the percent error e_k at the k'th iteration defined by

$$e_k \triangleq 100 \cdot \frac{||f-f_k||}{||f||} \qquad (17)$$

where $f \triangleq f(x,y)$ is the full scan (360 degrees) reconstructed image.

A summary of the *a priori* known facts and assumptions made about the image are given in Table I. Table II furnishes a summary of the experimental results.

Table I. Summary of *a priori* assumed constraints

a priori constraints	Actual
(1) Image support confined to rectangular region of length 124 pixels and width 103 pixels.	(1) Image support is elliptical (Figure 3).
(2) Gray levels f satisfy $0 \le f \le 0.4$	(2) Gray levels f satisfy $0 \le f \le 0.38$
(3) Energy over 128x128 square pixel field cannot exceed $\rho^2=284.000$	(3) Energy over 128x128 square pixel field is 282.74

Table II. Summary of significant results

Available View Range	Algorithm Name	Algorithm Description	Relaxation Parameters	Percent Error e_0	Percent Error e_{30}
[-45,45]	GP	$P_2P_1f_k=f_{k+1}$	$\lambda_1=\lambda_2=1.0$	52.419	47.511
	UNIRELAXL	$P_4P_2P_3P_1f_k=f_{k+1}$	$\lambda_1=\lambda_2=1.0$ $\lambda_3=\lambda_4=1.0$		42.057
[-67,67]	GP	$P_2P_1f_k=f_{k+1}$	$\lambda_1=\lambda_2=1.0$	45.000	22.203
	UNIRELAX	$P_2P_3P_1f_k=f_{k+1}$	$\lambda_1=\lambda_2=\lambda_3=1.0$		17.837
	RELAX	$T_2T_3T_1f_k=f_{k+1}$	$\lambda_1=\lambda_3=1.9995$ $\lambda_2=1.0$		16.184
[-80,80]	GP	$P_2P_1f_k=f_{k+1}$	$\lambda_1=\lambda_2=1.0$	41.361	15.485
	UNIRELAX	$P_2P_3P_1f_k=f_{k+1}$	$\lambda_1=\lambda_2=\lambda_3=1.0$		12.100
	RELAX	$T_2T_3T_1f_k=f_{k+1}$	$\lambda_1=\lambda_3=1.9995$ $\lambda_2=1.0$		9.352

a) Results for When Projection Data Is Limited to [-45°,45°]

In this case the reconstructed image at the end of 30 iterations is of low visual quality for all algorithms. Still the DFM reconstruction using UNIRELAXL (i.e. level constraints applied) restoration outperforms the DFM reconstruction using GP restoration. (See Table II)

b) Results for When Projection Data Is Limited to [-67°,67°]

In this case the three different restoration algorithms GP, UNIRELAX, and RELAX are separately combined with DFM reconstruction. The naive solution, which is merely inverse Fourier transforming the polar to Cartesian interpolated spectrum having zeroes for the entries corresponding to unavailable angular region (Figure 4) results in an error of 45 percent. In Figure 5 the naive solution is compared to reconstructions using GP, UNIRELAX and RELAX restorations. With the RELAX restoration an error less than 17 percent is reached at the end of 30 iterations and as can be seen from Figure 5 PRDF reconstruction incorporating UNIRELAX and RELAX restoration outperforms the reconstruction based on GP restoration.

c) Results for When Projection Data is Limited to [-80°,80°]

The naive reconstruction (e_o=42 percent) and the reconstructed images at the end of 30 iterations using RELAX, UNIRELAX and GP restorations are compared in Figure 6. As before, reconstructions using a posteriori restoration is superior to the naive reconstruction. The reconstruction by the RELAX restoration

M. Ibrahim Sezan and Henry Stark

TOMOGRAPHIC IMAGE RECONSTRUCTION FROM INCOMPLETE DATA BY USING CONVEX PROJECTIONS AND DIRECT FOURIER INVERSION

RECONSTRUCTION TOMOGRAPHIQUE A PARTIR DE DONNEES INCOMPLETES PAR PROJECTION CONVEXE ET INVERSION DIRECTE DE FOURIER

outperforms the reconstruction performed by the classical GP restoration. The superior performance of RELAX is especially evident in the reconstruction of the elliptical structure (note the obliterations in the GP case) and the reduced plume-like clouding from the tips of bright objects.

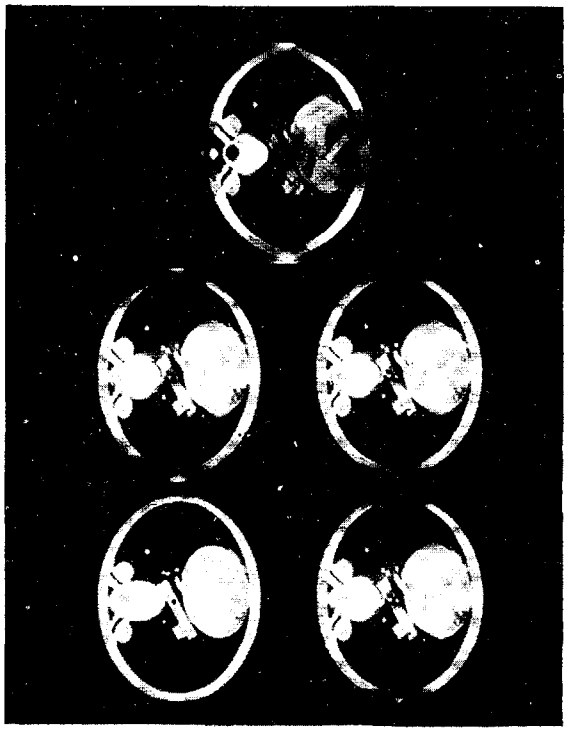

Figure 5. Reconstructions when projection data is limited to [-67°,67°]. Top: naive reconstruction then clockwise from upper left, GP, RELAX, UNIRELAX and full view data reconstruction.

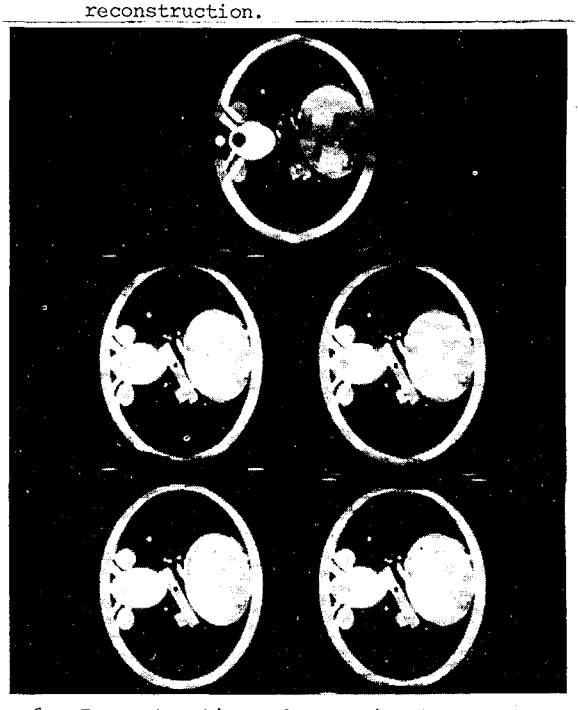

Figure 6. Reconstructions when projection data is limited to [-80°,80°]; Top: naive reconstruction; then clockwise from upper left: GP, RELAX, UNIRELAX and full view data reconstruction.

VI. APPLICATIONS IN NUCLEAR MAGNETIC RESONANCE (NMR) TOMOGRAPHY

In general PRDF is suitable for both medical and non-medical applications of tomographic image reconstruction from projections. Moreover it is also well suited for applications where the frequency spectrum of the image function is directly measured. Nuclear magnetic resonance (NMR) imaging is intrinsically a three-dimensional imaging modality. However by selective excitation [12] we can achieve tomographic imaging of the spatial nuclear magnetization distribution of a selected slice [12]. With saturation recovery pulse sequencing [12], the imaging equation i.e., the relation between the measured signal $S(t)$, and the equilibrium nuclear magnetization distribution $M_o(x,y,z)$, has the following form

$$S(t) = K \iint_{\Omega_{xy}} M_o(x,y)\ \exp[-i\gamma(G_x x+G_y y)t]dxdy \qquad (18)$$

where

$$M_o(x,y) = \int_{\Omega_z} R(z)\ M_o(x,y,z)dz$$

In Eq. (18) G_x and G_y are the x and y gradient field components, $R(z)$ is the response resulting from slice selection, γ is the gyromagnetic ratio, K is a constant, Ω_z and Ω_{xy} are the object supports in the z direction and in the selected slice respectively.

However, in practice data is sampled over a polar grid by taking $G_{x(k)}=G\cos\phi_k$ and $G_{y(k)}=G\sin\phi_k$ where $\phi_k = \frac{2\pi}{M}k$; $k=1,2,\ldots,M$. Then Eq. (18) becomes:

$$S_k(t) = K \iint_{\Omega_{xy}} M_o(x,y)\cdot \exp[-i\gamma G(x\cos\phi_k+y\sin\phi_k)t]dxdy\ ;$$

$$k=1,2,\ldots,M \qquad (20)$$

and after sampling $S_k(t)$ with interval $T=\Delta t$ the received signal is related to the nuclear magnetization by the following imaging equation

$$S_{nk} \triangleq S_k(n\Delta t)=K\iint_{\Omega_{xy}} M_o(x,y)\cdot\exp[-i\gamma Gn(x\cos\phi_k+y\sin\phi_k)\Delta t]dxdy$$

$$k=1,2,\ldots,M\ ,\ n=1,2,\ldots,N \qquad (21)$$

But S_{nk} is the 2-D Fourier transform of the nuclear magnetization $M_o(x,y)$ sampled at $(\gamma Gn\Delta t\cos\phi k, \gamma Gn\Delta t\sin\phi_k)$ or equivalently, at $(r_n\cos\phi_k, r_n\sin\phi_k)$, $k=1,2,\ldots,M$; $n=1,2,\ldots,N$ where $r_n \triangleq \gamma Gn\Delta t$. Therefore the Fourier spectrum of the image distribution (nuclear magnetization distribution of the selected slice) can be directly measured over a polar grid in the frequency domain. If complete spectrum information is available the direct Fourier inversion method (DFM) can be used to reconstruct the nuclear magnetization distribution. In case of limited-view measurements the missing spectrum can be restored via POCS prior to Fourier inversion. This restoration followed by Fourier inversion is indeed our PRDF reconstruction algorithm. Limited-view measurements are motivated by the desire for reduction of data collection time.

VII. CONCLUSIONS AND SUMMARY

In this paper we presented and applied a reconstruction algorithm (PRDF) that is synthesized from a recent restoration algorithm called projections onto convex sets (POCS) and from a direct Fourier inversion method (DFM) based on an exact polar to Cartesian interpolation formula. The PRDF algorithm is capable of performing reconstruction from angularly limited projection data. If the projection data is collected via fan beam geometry, rebinning can be applied prior to reconstruction to perform the conversion to equivalent

parallel beam projection data.

We also discussed the possibility of applying the PRDF algorithm to NMR tomography. Unlike X-ray tomography, NMR tomography yields the frequency spectrum of the image distribution directly over a polar grid in the frequency domain. This fact suggests that NMR imaging is a potential candidate for the interpolation and restoration phase of the PRDF algorithm.

REFERENCES

[1] D.C. Youla and H. Webb, "Image Restoration by the Method of Convex Projections: Part 1 - Theory", IEEE Trans. on Medical Imaging, Vol. MI-1, No. 2, October 1982.

[2] M.I. Sezan and H. Stark, "Image Restoration by the Method of Convex Projections: Part 2 - Applications and Numerical Results", IEEE Trans. on Medical Imaging, Vol. MI-1, No. 2, October 1982.

[3] H.K. Tuy, "An Algorithm for Incomplete Range of Views Reconstruction", Technical Digest of Topical Meeting on Signal Recovery and Synthesis with Complete Information and Partial Constraints, pp. FA1-1, FA1-4, Nevada, January 1983.

[4] Z. Opial, "Weak Convergence of the Sequence of Successive Approximations for Nonexpansive Mappings", Bull. Am. Math. Soc. 73, pp. 591-597, 1967.

[5] L.G. Gubin, B.T. Polyak and E.V. Raik, "The Method of Projections for Finding the Common Point of Convex Sets", U.S.S.R. Comput. Math. and Math. Phys., Vol. 7, No. 6, pp. 1-24, 1967.

[6] M.I. Sezan and H. Stark, "Image Restoration By Convex Projections in the Presence of Noise", Applied Optics, Vol. 22, September 15, 1983.

[7] A. Papoulis, "A New Algorithm in Spectral Analysis and Band Limited Extrapolation", IEEE Trans. on Circuits and Systems, Vol. CAS-22, pp. 735-742, 1975.

[8] H. Stark, J.W. Woods, I. Paul and R. Hingorani, "An Investigation of Computerized Tomography By Direct Fourier Inversion and Optimum Interpolation", IEEE Trans. Biomed. Eng., Vol. BME-28, pp. 496-505, July 1981.

[9] R.M. Lewitt, "Reconstruction Algorithms: Transform Methods", IEEE Proc. Vol. 71, No. 3, March 1983.

[10] H. Stark, "Sampling Theorems in Polar Coordinates", J. Opt. Soc. Amer., Vol. 69, Nov. 1979.

[11] H. Stark and M. Wengrovitz, "Comments and Corrections on the Use of Polar Sampling Theorems in CT", IEEE Trans. on Acoust., Speech and Signal Proc., Vol. ASSP-31, No. 5, October 1983.

[12] W.S. Hinshaw, A.H. Lent, "An Introduction to NMR Imaging: From the Bloch Equations to the Imaging Equation", IEEE Proc., Vol. 71, No. 3, March 1983.

ACKNOWLEDGEMENT

Many thanks are due to Dr. H. Tuy who supplied the thorax phantom projection data. We would also like to acknowledge our valuable technical discussions with him. This work is supported by National Science Foundation under Grant ECS-81-11264.